Friction Stir Welding and Processing V
Edited by: Rajiv S. Mishra, Murray W. Mahoney, and Thomas J. Lienert
TMS (The Minerals, Metals & Materials Society), 2009

FATIGUE CRACK GROWTH IN FRICTION STIR WELDED Ti-5111

P.S. Pao, R.W. Fonda, H.N. Jones, C.R. Feng, and D.W. Moon

Naval Research Laboratory, Washington, DC 20375, USA

Keywords: Friction stir welding, Fatigue crack growth, Microstructure, Titanium, Residual stresses.

Abstract

The effects of weld microstructure and weld speed on the fatigue crack growth kinetics of friction stir welded Ti-5111 were investigated. The FSW welds in Ti-5111 consist of very fine recrystallized grains, in contrast to coarse basketweave grains in the base plate. Fatigue crack growth rates are significantly lower and fatigue crack growth thresholds are significantly higher through the weld than those in the base plate. As the weld speed increases, the fatigue crack growth rates are progressively higher and fatigue crack growth thresholds lower through the weld. However, after stress-relief annealing, such differences in fatigue crack growth kinetics among different weld speeds no longer exist. Fatigue crack growth rates through post stress-relieved welds are higher than those in the base metal. The observed fatigue crack growth responses are discussed in terms of differences in crack tip microstructure, compressive residual stresses, crack closure, and crack deflection.

Introduction

Ti-5Al-1Sn-1Zr-1V-0.8Mo-0.1Si (Ti-5111) is a near-alpha titanium alloy in the 700 MPa yield strength class. Ti-5111 was developed as a lower cost substitute for Ti-6Al-2Nb-1Ta-0.8Mo (Ti-6211) with better producibility. Ti-5111 offers high strength, excellent corrosion resistance, good fracture toughness and stress-corrosion cracking resistance and is a good candidate for many structural applications in marine environments. Ti-5111 structures are typically joined by fusion welding techniques such as electron-beam, laser-beam, and gas-metal arc welding. Because of the high reactivity of molten titanium, oxygen can readily enter the weld. Interstitial oxygen, in relatively low concentration, has been known to significantly lower the stress-corrosion cracking resistance of titanium alloys [1]. Thus, conventional titanium fusion welding is typically performed in vacuum or with an inert gas shielding.

Friction stir welding (FSW), which was introduced by TWI in 1991, has emerged as a promising alternative to conventional fusion welding [2]. FSW is a solid-state welding process in which joining is achieved by the combined action of plastic deformation and frictional heat. Since the material to be joined stays below its melting point during FSW, the extent of oxidation and oxygen pick up is significantly reduced. Besides low oxygen pickup, FSW also offers many advantages over conventional fusion welding such as low weld distortion, easy automation, low defect population, environmental friendliness, lower cost, and the ability to join materials that are deemed unweldable by conventional fusion techniques. FSW has been gaining acceptance in the aerospace and transportation industries for joining aluminum alloys for application such as the Delta rocket and ship structures, primarily because the tools are readily available for these soft and low melting point alloys. Because titanium alloys have

Report Documentation Page

Form Approved
OMB No. 0704-0188

Public reporting burden for the collection of information is estimated to average 1 hour per response, including the time for reviewing instructions, searching existing data sources, gathering and maintaining the data needed, and completing and reviewing the collection of information. Send comments regarding this burden estimate or any other aspect of this collection of information, including suggestions for reducing this burden, to Washington Headquarters Services, Directorate for Information Operations and Reports, 1215 Jefferson Davis Highway, Suite 1204, Arlington VA 22202-4302. Respondents should be aware that notwithstanding any other provision of law, no person shall be subject to a penalty for failing to comply with a collection of information if it does not display a currently valid OMB control number.

1. REPORT DATE	2. REPORT TYPE	3. DATES COVERED
FEB 2009		**00-00-2009 to 00-00-2009**

4. TITLE AND SUBTITLE	5a. CONTRACT NUMBER
Fatigue Crack Growth in Friction Stir Welded Ti-5111	5b. GRANT NUMBER
	5c. PROGRAM ELEMENT NUMBER
6. AUTHOR(S)	5d. PROJECT NUMBER
	5e. TASK NUMBER
	5f. WORK UNIT NUMBER
7. PERFORMING ORGANIZATION NAME(S) AND ADDRESS(ES) **Naval Research Laboratory,Washington,DC,20375**	8. PERFORMING ORGANIZATION REPORT NUMBER
9. SPONSORING/MONITORING AGENCY NAME(S) AND ADDRESS(ES)	10. SPONSOR/MONITOR'S ACRONYM(S)
	11. SPONSOR/MONITOR'S REPORT NUMBER(S)

12. DISTRIBUTION/AVAILABILITY STATEMENT
Approved for public release; distribution unlimited

13. SUPPLEMENTARY NOTES
See also ADM002300. Presented at the Minerals, Metals and Materials Annual Meeting and Exhibition (138th)(TMS 2009) Held in San Francisco, California on February 15-19, 2009. Sponsored in part by the Navy.

14. ABSTRACT
The effects of weld microstructure and weld speed on the fatigue crack growth kinetics of friction stir welded Ti-5111 were investigated. The FSW welds in Ti-5111 consist of very fine recrystallized grains, in contrast to coarse basketweave grains in the base plate. Fatigue crack growth rates are significantly lower and fatigue crack growth thresholds are significantly higher through the weld than those in the base plate. As the weld speed increases, the fatigue crack growth rates are progressively higher and fatigue crack growth thresholds lower through the weld. However, after stress-relief annealing, such differences in fatigue crack growth kinetics among different weld speeds no longer exist. Fatigue crack growth rates through post stressrelieved welds are higher than those in the base metal. The observed fatigue crack growth responses are discussed in terms of differences in crack tip microstructure, compressive residual stresses, crack closure, and crack deflection.

15. SUBJECT TERMS

16. SECURITY CLASSIFICATION OF:			17. LIMITATION OF ABSTRACT	18. NUMBER OF PAGES	19a. NAME OF RESPONSIBLE PERSON
a. REPORT **unclassified**	b. ABSTRACT **unclassified**	c. THIS PAGE **unclassified**	**Same as Report (SAR)**	**10**	

higher strength and toughness, the tooling required for FSW is much more demanding and challenging.

Friction stir welding has been shown to produce significantly different weld region microstructures when compared to the base plate [3-9]. The FSW weld nugget region in aluminum alloys, steels, and titanium alloys typically consists of very fine equiaxed grains. Previous investigations have indicated that fatigue crack growth is affected by grain size, with fatigue crack growth rates significantly higher through fine grain materials [10,11]. Residual stresses developed during FSW have been shown to be substantial and can improve fatigue crack growth resistance [3,7,8]. However, the effect of FSW weld microstructure and residual stresses on fatigue crack growth kinetics of Ti-5111 have not been systematically investigated.

In this paper, the microstructures, microhardness, and fatigue crack growth kinetics through FSW Ti-5111 weld region produced under various welding speeds were studied and were compared to those of base metal.

Experimental Procedures

Both 12.7 mm and 6.3 mm thick Ti-5111 plates were used in this study. Single-pass FSW butt joints were prepared at the Edison Welding Institute using a tungsten based tool. The rotational speed was 225 rpm. The weld speed was 51 mm/min for the 12.7 mm thick plate (Weld 1). For the 6.3 mm thick plates, two weld speeds, 25.4 mm/min (Weld 2) and 102 mm/min (Weld 3), were used. Transverse cross section microhardness maps were obtained for these welds. Optical microscopy was used to examine microstructures in the weld nugget and base metal.

While the two 6.3 mm thick Ti-5111 welds, Weld 2 and Weld 3, were defect-free, radiographic examinations indicated the presence of wormholes in the 12.7 mm thick Ti-5111 Weld 1. Most of these wormholes were located near the bottom of the plate. As such, 3.2 mm of material was machined off from both the top and the bottom of Weld 1 to remove these defects. Thus, only the middle 6.3 mm-thick portion of Weld 1 plate was used for fatigue crack growth studies.

5.8 mm thick, 50.8 mm-wide compact tension (CT) fracture mechanics type specimens were used in this study. The notch direction and the crack growth direction were parallel to the welding direction. For added constraint, 5% side grooves were machined on the specimen surfaces. The notch of the CT specimen was positioned at the center of weld. For comparison, CT specimens with the notch located in the base plate region far from the weld were machined from 6.3 mm thick Ti-5111 plate (W3 plate). To determine the effect of weld residual stresses on fatigue crack growth, half of the as-welded and base plate CT specimens were stress-relief annealed in vacuum at 1100 °C for 2 hours, followed by a rapid cooling in flowing argon to ambient temperature. All fatigue crack growth tests were carried out in ambient air (20°C and 42% relative humidity) at a cyclic frequency of 10 Hz and a stress ratio, R, of 0.1. A compliance technique was used to continuously monitor the fatigue crack growth. Post-fatigue fracture surfaces were examined by scanning electron microscopy (SEM) and the average fracture roughness was determined by an optical profilometer.

Results and Discussion

Microstructural Analysis and Microhardness Map

The microstructural characteristics and microhardness maps for Ti-5111 FSW W1, W2, and W3 are similar and only W1 is discussed in detail here. The transverse cross section macrograph and the microhardness map across the mid-thickness of the weld nugget shown in Figs. 1 and 2 are taken from the bead-on plate weld on the same 12.7 mm thick Ti-5111 plate using identical welding parameters and tools as those of Weld 1. The low magnification transverse cross section of 12.7 mm thick Ti-5111 FSW weld is shown in Fig. 1. Fig.1 reveals only two distinct regions, a fine-grained weld nugget region surrounded by a coarse grained base plate region. The base plate consists of very large grains, particularly in the center of the plate where grains as large as 8 mm were present. The large grains in the base plate clearly reveal the boundary between the base plate and the weld nugget. Unlike FSW aluminum alloys and FSW steels where the transition from base plate microstructure to weld nugget microstructure is gradual and is comprised of several zones such as the thermomechanical-affected zone (TMAZ) and heat-affected zone (HAZ), the transition in FSW titanium is abrupt as shown in Fig.1 and no apparent transitional zone is observed. A previous study on the microstructural evolution in Ti-5111 confirmed that the transition from the base plate to weld nugget was abrupt with a transition zone width on the order of only several hundreds micrometers [5]. Because of this unique "two-zone" microstructure, fatigue crack growth studies in FSW Ti-5111 are concentrated on comparing fatigue crack growth kinetics through the fine-grained FSW nugget region to that through the base plate.

Figure 3a shows a typical optical micrograph taken from the base plate. It consists of coarse Widmanstatten structure with many colonies in which α plates align in the same orientation. This base plate microstructure suggests that the plate has been hot rolled above the β transus followed by an α/β anneal. Most of the prior β grains are several millimeters in size with some exceeding 8 mm. Figure 3b shows the fine equiaxed microstructure in the FSW nugget region. In contrast to the coarse grains found in base plate, the average grain size in the FSW nugget region is only about 30 μm. Fine α plates, often in the same orientation, precipitate in the prior beta grains and the alpha phase decorating the grain boundaries. This microstructure clearly indicates that the temperature excursion during friction stir welding has exceeded the beta transus temperature. Furthermore, the very fine equiaxed grain structure observed in the nugget region suggests that the time spent above the beta transus is short, as beta grains would otherwise coarsen rapidly.

The microhardness map and microhardness scan across the mid-thickness of the transverse section of the 12.7 mm thick Ti-5111 FSW weld is shown in Fig. 2. As shown in Fig. 2, the microhardness across the coarse grain base plate region varies between 260 and 360 HVN, while the fine equiaxed grain nugget region exhibits more uniform microhardness in the range of 300 to 320 HVN. Thus, unlike FSW HSLA-65 steel which shows a significant overmatch in the weld nugget, and FSW Al 7050 which shows a considerable undermatch, the difference in microhardness between the base plate and weld nugget of Ti-5111 is small [3,8].

Thus, the major microstructural characteristics in FSW Ti-5111 is the conversion of coarse Widmanstatten structure of the base plate to fine equiaxed grains in the nugget.

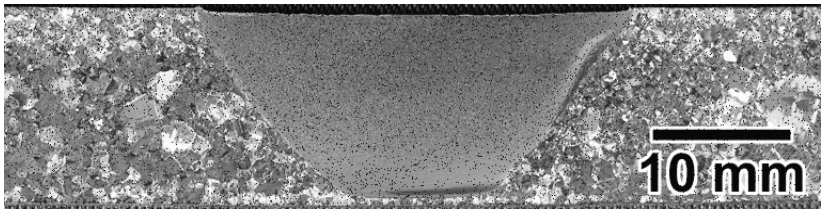

Fig. 1 Transverse cross section of the Ti-5111 FSW weld.

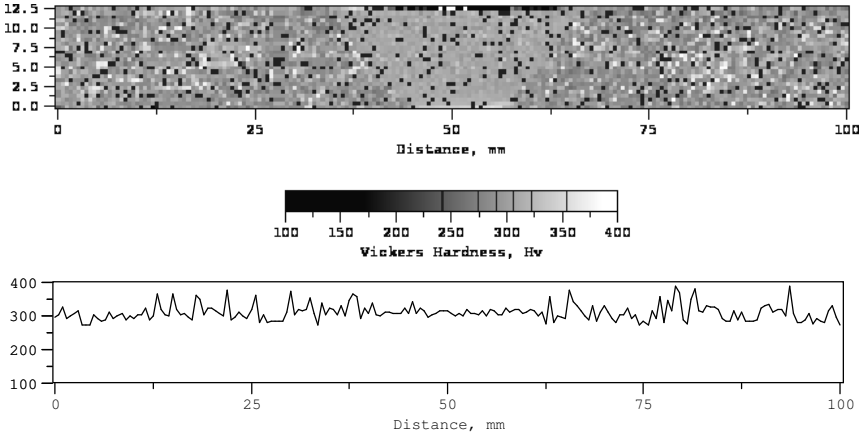

Fig. 2 Microhardness map and microhardness scan across the mid-thickness of the Ti-5111 weld.

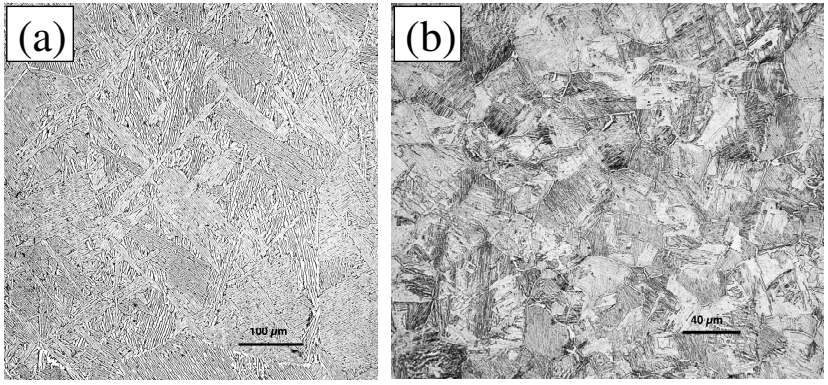

Fig.3 Optical micrographs from (a) the base plate and (b) weld nugget of FSW W1 plate.

Fatigue Crack Growth

The fatigue crack growth kinetics through the Ti-5111 FSW weld nugget regions and through the base plate are shown in Fig. 4. For comparison, Fig. 4 also includes previous fatigue crack growth rate data from 25 mm thick Ti-5111 plate that was not subjected to welding conditions. As shown in Fig. 4, irrespective of the plate thickness, the fatigue crack growth rate through the weld nugget is highest in the fastest weld speed plate W3, followed by middle weld speed plate W2, and is lowest in slowest weld speed plate W1. The fatigue crack growth threshold stress intensity, ΔK_{th} below which the crack will not propagate, is lowest in fastest weld speed plate W3 and is highest in slowest weld speed plate W1. The difference in fatigue crack growth rates through the weld nugget regions of W1, W2, and W3 plates progressively diminishes as the stress intensity, ΔK, increases. Above a ΔK of 20 MPa $\sqrt{m}$, fatigue crack growth rates through these weld nuggets are comparable. The fatigue crack growth rates through the base plate and the weld nugget regions of W3 plate are comparable and are substantially higher than those through the weld nugget regions of W1 and W2 plates.

The fatigue crack growth rates obtained from the 25.4 mm thick Ti-5111 plate, at similar ΔK levels, are higher than those from the base plate region of W3 plate used in this study. The 25.4 mm thick Ti-5111 plate used in a previous fatigue study did not experience welding conditions and, thus, is free from welding-induced residual stresses [12]. It is believed that, during FSW of the 6.3 mm thick Ti-5111 plate, the high clamping loads and the thermal excursion may be enough to introduce significant, though small, residual stresses in the base plate region. The presence of these small residual stresses in the base plate region of 6.3 mm thick W3 plate can effectively reduce the crack tip driving force and result in slightly lower fatigue crack growth rates and higher fatigue crack growth thresholds, when compared to those from the residual stress-free 25.4 mm thick Ti-5111 plate used in previous study.

The better fatigue crack growth performance through the weld nugget regions, as manifested by the lower fatigue crack growth rates and higher fatigue crack growth thresholds, is believed to be caused by the presence of compressive residual stresses in the weld plates. The presence of compressive residual stresses and thus the better fatigue crack growth resistance through the FSW weld nugget regions also have been reported for FSW HSLA-65 steel and FSW aluminum alloys [3,7,8]. To verify the presence of residual stresses in FSW Ti-5111 plates and to determine the extent of their influence on fatigue crack growth, CT fatigue specimens made from the FSW nugget regions as well as from the base plate region were stress-relief annealed. The fatigue crack growth kinetics obtained from stress-relief annealed CT specimens is compared in Fig. 5.

After stress-relief annealing, the fatigue crack growth kinetics obtained from the base plate region of W3 plate, as shown in Fig. 5, are identical to that obtained from the residual stress-free 25.4 mm thick Ti-5111 plate used in the previous study. This suggests that residual stresses were indeed present in the base plate region of plate W3. Relieving these residual stresses causes the fatigue crack growth response of the base plate region of Ti-5111 FSW weldments to approach that of the residual stress-free Ti-5111.

Figure 6 directly compares the fatigue crack growth kinetics, before and after residual stress-relief annealing, through the weld nugget of slowest weld speed W2 plate. The residual stresses have considerable beneficial effect, as the fatigue crack growth rates of as-welded material are significantly lower than those from the stress-relieved material. Furthermore, the nugget region fatigue crack growth threshold decreases from about 12 to 3 MPa$\sqrt{m}$ following the stress-relief annealing. Of course, after the stress-relief annealing, this beneficial effect is gone.

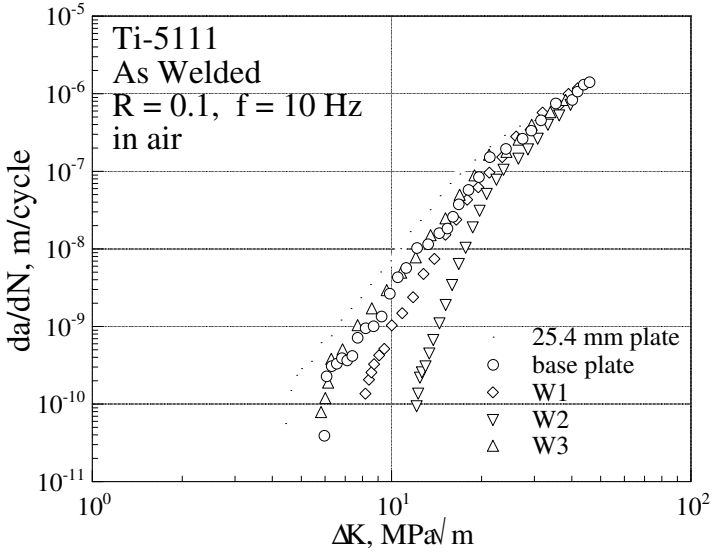

Fig. 4 Fatigue crack growth kinetics obtained from as-welded Ti-5111.

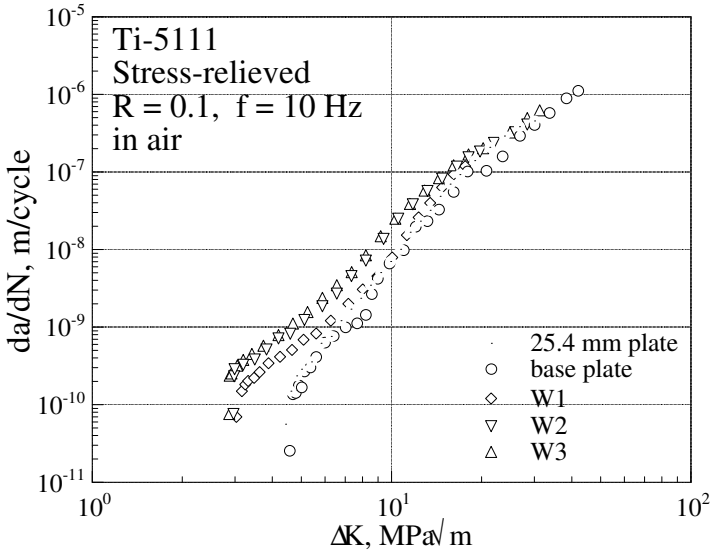

Fig. 5 Fatigue crack growth kinetics obtained from stress-relieved Ti-5111.

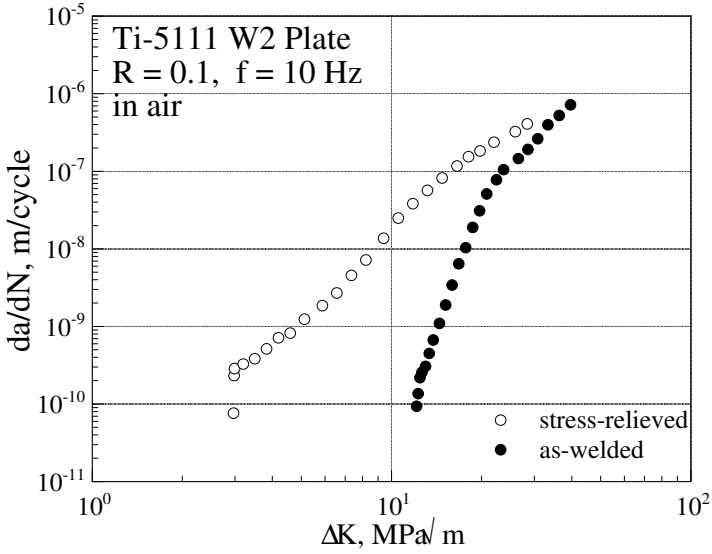

Fig. 6 Comparison of through weld nugget fatigue crack growth kinetics in as-welded and residual stress-relieved Ti-5111 W2 plate.

The fatigue crack growth rate curves for the stress relieved weld nuggets all shift to the left of that obtained from the residual stress-free base plate, as shown in Fig. 5. In stress-relieved weld nugget regions, the fatigue crack growth rates are higher and the fatigue crack growth thresholds are significantly lower when compared to those from the annealed base plate. Since both weld nugget and base plate CT specimens are annealed and contain no or little residual stresses, the difference in fatigue crack growth response, as shown in Fig. 5, can be attributed only to the difference in crack tip microstructure. As shown in Fig. 1, the nugget region contains very fine grains that are about two orders-of-magnitude smaller than the coarse grains found in the base plate. This difference in crack tip grain size results in a significant difference in fracture surface morphology and fracture surface roughness, particularly in the near-threshold region.

Figure 7 shows near-threshold fracture surface morphologies taken from weld nugget and base plate. As shown in Fig. 7a, the fracture surface obtained from the coarse-grained base plate is very rough and the fracture path is highly tortuous as compared to the weld nugget's much smoother fracture surface appearance and straighter fracture path shown in Fig. 7b. Average fracture roughness, as measured by optical profilometer, for base plate and weld nugget regions are 15 μm and 2 μm, respectively. Rougher fracture surfaces can cause roughness-induced crack closure and prematurely close the crack during the unloading cycle. This would result in the reduction of crack tip driving force, •K, and lower fatigue crack growth rates, as is the case for the coarse-grained base plate shown in Fig. 5. In addition, the base plate's tortuous fracture paths would also cause crack deflection and further reduce the effective crack tip driving force

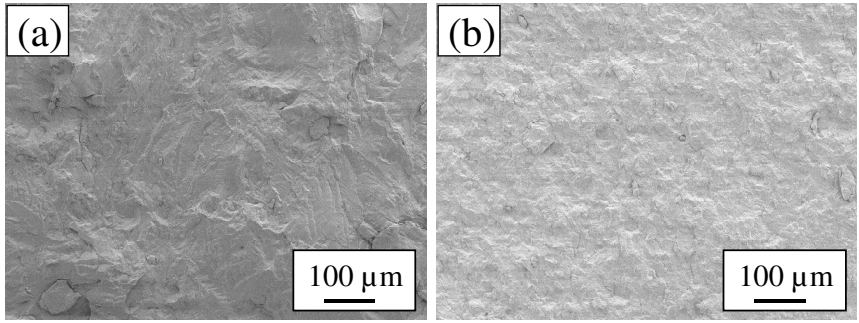

Fig. 7 Near-threshold fracture surface morphology taken from stress-relieved W3 plate, (a) base plate region and (b) weld nugget region.

and fatigue crack growth rates [13]. Thus, the weld nugget regions' higher fatigue crack growth rates and lower fatigue crack growth thresholds can be attributed directly to their fine grain sizes, which result in diminished crack closure and a low degree of crack deflection.

The fatigue crack growth rate curve taken from the weld nugget before residual stress-relief annealing, as shown in Fig. 4, progressively shifts to the left as weld speed increases. That is, at comparable •K, the fatigue crack growth rate through the weld nugget is the highest in the fastest weld speed W3 plate (102 mm/min) and is the lowest in slowest weld speed W1 plate (25.4 mm/min). The fatigue crack growth threshold goes the other way and is lowest in the fastest weld speed plate and highest in the slowest weld speed plate. Such a fatigue crack growth kinetics dependence on weld speed is believed to be caused by the difference in residual stresses, which is the result of different heat inputs during welding. Slower weld speeds correspond to hotter welding conditions, which could increase the residual stresses. Large residual stresses present in the slow weld speed plate can lower the effective •K and reduce the fatigue crack growth rates. When such residual stresses are removed by stress-relief annealing, then the difference in fatigue crack growth kinetics among plates with various weld speeds would be greatly diminished, as demonstrated in Fig. 5.

It is interesting to note that, prior to residual stress-relief annealing as shown in Fig. 4, the fatigue crack growth kinetics obtained from the nugget region of the fastest weld speed Ti-5111 W3 plate is identical to that from the base plate region of the same plate. The weld nugget and base plate have very dissimilar grain sizes and must also have very different residual stress distributions. However, the fatigue crack growth response in FSW Ti-5111 is primarily dictated by two parameters, crack tip microstructure and residual stress distribution. On the one hand, the weld nugget region's fine grain size would result in smoother fracture surface morphology, low crack closure level, and a low degree of crack deflection, all of which would enhance fatigue crack growth. On the other hand, the high compressive residual stresses present in the FSW weld nugget would reduce the effective •K and lower the fatigue crack growth rates. It is coincidental that the effects of grain size and residual stresses, which have opposite influences on fatigue crack growth in FSW Ti-5111 cancel each other out and result in an apparent identical fatigue crack growth kinetics, as observed for fatigue crack growth through the weld nugget and base plate of W3 plate.

Conclusions

1. The weld nugget consists of a single weld region with a grain size significantly smaller than that of the base plate.
2. The fatigue crack growth kinetics through the weld nugget is strongly affected by the presence of residual stresses and the crack tip microstructures.
3. In the as-welded condition, the fatigue crack growth rates are significantly lower and fatigue crack growth thresholds are significantly higher through the weld than those in the base plate.
4. As the weld speed increases, the fatigue crack growth rates become progressively higher and fatigue crack growth thresholds lower through the weld. However, after stress-relief annealing, such differences in fatigue crack growth kinetics among different weld speeds greatly diminishes.
5. Fatigue crack growth rates through post stress-relieved welds are higher than those in the base metal. This can be attributed to the weld nugget's lower crack closure level and lower degree of crack deflection.

Acknowledgements

The authors would like to acknowledge financial support from the Naval Research Laboratory under the auspices of the Office of Naval Research. We also would like to thank Ernie Czyryca of Naval Surface Warfare Center at Carderock for providing information on stress-relief.

References

1. P.S. Pao, M.A. Imam, H.N. Jones, R.A. Bayles, and C.R. Feng, "Effect of Oxygen on Stress-Corrosion Cracking and Fatigue Crack Growth of Ti-6211," in the Proceedings of the 11th World Conference on Titanium, The Japan Institute of Metals, pp. 279-282 (2007).
2. W.M. Thomas, E.D. Nicholas, J.C. Needham, M.G. Nurch, P. Temple-Smith, and C.J. Dawes, "Friction Stir Butt Welding," International Patent Application No. PCT/GB92/02203, GB Patent Application No. 9125978.8 (1991), and U.S. Patent No. 5,460,317 (1995).
3. P.S. Pao, R.W. Fonda, H.N. Jones, C.R. Feng, and D.W. Moon, "Friction Stir Welding of HSLA-65 Steel," in Friction Stir Welding and Processing IV (Eds. R.S. Mishra, M.W. Mahoney, T.J. Lienert, and K.V. Jata), pp. 243-251, The Minerals Metals, and Materials Society, 2007.
4. M. Posada, J. DeLoach, A.P. Reynolds, R.W. Fonda, and J.P. Halpin, "Evaluation of Friction Stir Welded HSLA-65," in Proceedings of the Fourth International Symposium on Friction Stir Welding, TWI Ltd., S10A-P3 (2003).
5. R.W. Fonda, K.E. Knipling, C.R. Feng, and D.W. Moon, "Microstructural Evolution in Ti-5111 Friction Stir Welds," in Friction Stir Welding and Processing IV (Eds. R.S. Mishra, M.W. Mahoney, T.J. Lienert, and K.V. Jata), pp. 295-301, The Minerals Metals, and Materials Society, 2007.
6. C.G. Rhodes, M.W. Mahoney, W.H. Bingel, R.A. Spurling, and C.C. Bampton, "Effects of Friction Stir Welding on Microstructure of 7075 Aluminum," *Scripta Materialia*, 36 (1997), 69-75.
7. K.V. Jata, K.K. Sankaran, and J.J. Ruschau, "Friction-Stir Welding Effects on Microstructure and Fatigue of Aluminum Alloy 7050-T7451," *Met Mat Trans A*, 31A (2000), 2181-2192.
8. P.S. Pao, S.J. Gill, C.R. Feng, and K.K. Sankaran, "Corrosion-fatigue crack growth in friction stir welded Al 7050," *Scripta Materialia* 45 (2001), 605-612.
9. J. Corral, E.A. Trillo, Y. Li, and L.E. Murr, "Corrosion of Friction-Stir Welded Aluminum Alloys 2024 and 2195," *J Mat Sci Letters*, 19 (2000), 2117-2122.
10. P.S. Pao, H.N. Jones, S.F. Cheng, and C.R. Feng, "Fatigue Crack Propagation in Ultrafine Grained Al-Mg Alloy," International Journal of Fatigue, Vol. 27, 10-12, p. 1164(2006).

11. T. Hanlon, Y.N. Kwon, and S. Suresh, “Grain Size Effects on the Fatigue Response of Nanocrystalline Metals,” *Scripta Materialia*, 49 (2003), 675-680.
12. P.S. Pao, S.J. Gill, M.A. Imam, C.R. Feng, and R.A. Bayles, “Stress-Corrosion Cracking and Corrosion Fatigue Resistance in Ti-5111 and VLI Ti-6Al-4V,” in Ti-2003 Science and Technology, Wiley-VCH, pp. 2083-2090 (2004).
13. S. Suresh, “Fatigue of Materials,” Cambridge University Press (1992).